MicroRNA Overexpression screen reveals a noncanonical role of CDK2 in regulating neutrophil migration

Alan Y. Hsu[1], Decheng Wang[1,2], Sheng Liu[3,4], Justice Lu[1], Ramizah Syahirah[1], David A. Bennin[5], Anna Huttenlocher[5,6], Jun Wan[3,4,7], Qing Deng[1,8,9*]

1. Department of Biological Sciences, Purdue University, West Lafayette, IN 47907 USA
2. Medical College of China Three Gorges University, Yichang, Hubei, 443002 PR China
3. Department of Medical and Molecular Genetics, Indiana University School of Medicine, Indianapolis, IN 46202 USA
4. Collaborative Core for Cancer Bioinformatics, Indiana University Simon Cancer Center, Indianapolis, IN 46202 USA
5. Department of Medical Microbiology and Immunology, University of Wisconsin-Madison, Madison, WI, USA.
6. Department of Pediatrics, University of Wisconsin-Madison, Madison, WI, USA.
7. Center for Computational Biology and Bioinformatics, Indiana University School of Medicine, Indianapolis, IN 46202 USA
8. Purdue Institute for Inflammation, Immunology, & Infectious Disease, Purdue University, West Lafayette, IN 47907 USA
9. Purdue University Center for Cancer Research, Purdue University, West Lafayette, IN 47907 USA

*Corresponding author:
G231 Biological Sciences
Purdue University
915 W. State Street
West Lafayette, IN 47907
Tel: 765-494-0423
Fax: 765-494-0876
qingdeng@purdue.edu

Abstract

Neutrophil migration is essential for inflammatory responses to kill pathogens and cause tissue injury. To discover novel therapeutic targets that modulate neutrophil migration, we performed a neutrophil-specific microRNA overexpression screen in zebrafish, and identified eight microRNAs as potent suppressors of neutrophil migration. Among those, *miR-199* decreases neutrophil chemotaxis in zebrafish and human neutrophil-like cells. Intriguingly, in terminally differentiated neutrophils, *miR-199* alters the cell cycle-related pathways and directly suppresses *cyclin-dependent kinase 2* (*cdk2)*, whose known activity is restricted to cell cycle progression and cell differentiation. Inhibiting CDK2, but not DNA replication, disrupts cell polarity and chemotaxis of zebrafish neutrophils. Chemotaxis of primary human neutrophils are also reduced by CDK2 inhibition. Furthermore, *miR-199* overexpression or CDK2 inhibition significantly improves the outcome of lethal systemic inflammation challenges in zebrafish. Together, our results reveal previously unknown functions of *miR-199* and CDK2 in regulating neutrophil migration and provide new directions in alleviating systemic inflammation.

Introduction

Neutrophils are the first cells recruited to an immune stimulus stemming from infection or sterile injuries via a mixture of chemoattractant cues[1]. In addition to eliminating pathogens, neutrophils coordinate the overall inflammation response by causing tissue damage and modulating the activation of other immune cells. Over amplified or chronic neutrophil recruitment directly leads to autoimmune diseases including rheumatic arthritis, diabetes, neurodegenerative diseases, and cancer[2]. Dampening neutrophil recruitment is a strategy to intervene neutrophil-orchestrated chronic inflammation[3]. Despite intensive research over the past several decades, clinical studies targeting neutrophil migration have been largely unsuccessful, possibly due to the prominent redundancy of adhesion receptors and chemokines. Additional challenges lie in the balance of dampening detrimental inflammation while preserving immunity[4]. Neutrophil migration is governed by spatially and temporally complex dynamic signaling network[5]. Immune cells use both mesenchymal migration (adhesive migration on substrate) and amoeboid migration (actin protrusion driven by weak substrate interaction) to infiltrate tissue using distinct signaling molecules[6, 7]. Extensive research is required to understand the machinery regulating neutrophil recruitment, which can lead to the development of exogenous inhibitors for clinical use.

MicroRNAs (miRNAs) are short (20-22 nucleotides) conserved non-coding RNAs that are epigenetic regulators of the transcriptome. By binding primarily to the 3´UTRs of their target transcripts and recruiting the RNA-induced silencing complex, miRNAs down-regulate gene expression[8]. miRNAs are generally fine-tuners that suppress gene expression at modest levels, and also master regulators that target the expression of a network of genes[9]. Recently, miRNAs and anti-miRNAs have been used in clinical trials to treat cancer and infection [10]. In addition, they have been used as tools to screen and identify the underlying mechanisms of diseases and cell behavior[11, 12]. In immune cells, an in vivo functional screen of microRNA was performed to identify microRNAs that regulate B cell tolerance[13]. In neutrophils, the functions of the highly expressed microRNAs *miR-223*[14] and *miR-142*[15] have been well characterized. However, other miRNAs and their targets as regulators of neutrophil recruitment remain largely unknown. The absence of this knowledge might lead to missed opportunities in harnessing microRNAs and their targets in restraining neutrophilic inflammation.

The zebrafish is a suitable model organism to study neutrophil biology. They have an evolutionarily conserved innate immune system, including the phagocytes and their signaling molecules including miRNAs[15, 16]. The transparent property of zebrafish embryos enables noninvasive imaging of neutrophil behavior under physiological conditions[17, 18]. Additionally, high fecundity and established genetic tools make zebrafish an ideal platform for genetic screens and drug discovery[19].

We have previously established a system to express individual miRNAs in zebrafish neutrophils to assess their function *in vivo*[20]. Here we performed a miRNA overexpression screen and identified *miR-199* as a novel regulator of neutrophil chemotaxis. Through *miR-199* target analysis, we identified the canonical cell cycle related gene *cdk2* as a new regulator of neutrophil migration. Overexpression of *miR-199* or inhibition of *cdk2* in neutrophils improved survival upon infection and sterile inflammatory challenges. Our results were further validated in human neutrophil-like cells and primary human neutrophils, supporting the evolutionary conservation of *miR-199* and Cdk2 in vertebrae neutrophil biology. Our discovery expands our current understanding of neutrophil migration and suggests a novel strategy to manage neutrophilic inflammation.

Results

Identification and characterization of miRNAs that regulate neutrophil recruitment

As a first step to understand microRNA mediated gene regulation in zebrafish neutrophils, we sequenced microRNAs in zebrafish neutrophils sorted from 3 day old embryos. Consistent with previous reports in human and mice, *miR-223* and *miR-142* were among the microRNAs highly expressed in zebrafish neutrophils (Fig. 1a, b and Dataset 1). As a control, we sequenced microRNAs in the immotile epical keratinocytes and indeed detected a distinct profile (Fig.1c, d). We next performed a functional genetic screen to identify a set of miRNAs overexpression of which moderates neutrophil migration (Supplementary Fig. 1). Forty-one microRNAs with lower expression levels compared with the whole embryo or keratinocytes were selected. Individual miRNA candidates were cloned and transiently expressed in zebrafish neutrophils, together with a fluorescent reporter gene. The miRNAs whose overexpression resulted in an over 50% reduction in neutrophil recruitment to infection sites were selected (Dataset 2). We generated transgenic zebrafish lines stably expressing the eight miRNAs that passed the initial screen. To rule out potential artifacts associated with the transgene integration sites, more than two independent founders were obtained for each line. In seven out of the eight lines, reduced neutrophil recruitment to ear infection sites were detected, regardless of the choice of the founder (Fig. 1e). Using a tailfin amputation inflammatory model, neutrophil recruitment was significantly inhibited in all eight lines (Fig. 1f and Dataset 3), concluding that the microRNA overexpression screen faithfully represented microRNAs which could modulate neutrophil migration. A microRNA characterized in our previous work, *miR-722*, served as a positive control[20]. Among the eight newly identified miRNAs, *miR-146* is a known suppressor of immune cell activation[21], whereas the other 7 miRNAs have not been characterized for their roles in neutrophilic inflammation or migration. The overexpression of *miR-199-3* resulted in the most robust inhibition in both models (Fig. 1e-j) and therefore was selected for further characterization.

***miR-199-3* overexpression inhibits neutrophil motility and chemotaxis.**

To characterize the zebrafish lines *Tg(lyzC: Dendra2-miR-199-3)*^{pu19} and *Tg(lyzC:Dendra2-vector)*^{pu7}, hereby referred as *miR-199* and vector lines, we first isolated their neutrophils and performed miRNA RT-qPCR to confirm the *miR-199* overexpression in the *miR-199* line (fig. 2A). The levels of two abundant neutrophil miRNAs, *miR-223* and *let-7e*, were not affected, showing that the overexpression did not disrupt physiological microRNA levels. Total neutrophil numbers in embryos were comparable between the two lines, suggesting that the observed decreased neutrophil recruitment was not an artifact of reduced neutrophil numbers (Fig. 2b, c). In addition to defective recruitment to inflammatory sites, the velocity of neutrophil spontaneous motility in the head mesenchyme was significantly decreased in the *miR-199* line (Fig 2d, e and Video S1), whereas their directionality was not affected (Fig. 2f). The sequences of the mature zebrafish and human *miR-199-5p* isoforms are identical (Fig. 3c).We therefore sought to determine whether *MIR-199* inhibits human neutrophil migration. We used *MIR-100*, whose overexpression did not result in any phenotype in the initial screen, as a negative control. We expressed *MIR-199a*, *MIR-100* or the vector alone under the control of a Tet Responsive Element in HL-60 cells, a myeloid leukemia cell line that can be differentiated into neutrophil-like cells as our model[22] (Supplementary Fig. 2a). *MIR-100* and *MIR-199* were individually induced in the respective lines without affecting cell differentiation, cell death or the expression of two other miRNAs, *MIR-223* and *LET-7* (Fig. 2g and Supplementary Fig. 2b-d). The cells were then allowed to migrate towards N-Formylmethionyl-leucyl-phenylalanine (fMLP) in transwells. Only the cells overexpressing *MIR-199*, but not the vector control or cells overexpressing *MIR-100*, displayed significant defects in chemotaxis (Fig. 2h). Together, our results show that overexpression of *MIR-199* inhibits neutrophil migration in both zebrafish and human cell models.

miR-199 suppresses the expression of cell cycle-related genes including *cdk2*

To understand the underlying molecular mechanism of how *miR-199* regulates neutrophil migration, neutrophils from the *miR-199* or vector lines were isolated and their transcripts subjected to RNAseq. Transcripts that were downregulated upon *miR-199* overexpression[23] were subjected to further analysis (Fig. 3a and Dataset 4). To our surprise, the top 10 pathways associated with the downregulated transcripts are related to cell cycle processes (Fig. 3b and Dataset 5). This result was surprising because neutrophils are known to be terminally differentiated, non-proliferative, and have exited the cell cycle[24]. To validate the RNAseq results, we selected 5 genes, *cdk2, cdk5, cdca8, kif14,* and *mcm5,* which were significantly downregulated, and confirm their reduced transcript levels in the *miR-199* line using RT-qPCR (Fig. 3c). The zebrafish orthologue of *IKBKB*, a known target of human *MIR-199*[25] and a critical component in the NF-κB pathway, was also downregulated, supporting the conservation of microRNA-target interactions in zebrafish. The level of cyclin dependent kinase 1 (*cdk1*) mRNA was not altered. The protein sequence of CDK2 is more than 90% identical between zebrafish and human, and both 3´ UTRs contain predicted *miR-199-5p* binding sites (Fig. 3d). To demonstrate direct targeting of *cdk2* mRNAs by *miR-199-5p*, we performed dual-luciferase reporter assays. *miR-199* significantly reduced the relative luciferase activity controlled by both the human and zebrafish *cdk2* 3´UTRs but did not show the repression of luciferase activity when the predicted binding sites were mutated (Fig. 3e). These results indicate that *miR-199* suppresses classical cell cycle pathways in neutrophils and directly targets *cdk2* in both zebrafish and humans.

Pharmacological inhibition of Cdk2 decreases neutrophil motility and chemotaxis

CDK2 is expressed and active in human neutrophils[26]. To test whether *cdk2* regulates neutrophil migration, we used NU6140[27], a CDK2 specific inhibitor. At a concentration of 100 µM, NU6140 did not affect zebrafish survival or neutrophil numbers (Supplementary Fig. 3). As a control for cell cycle progression and DNA replication, we used a mixture of Aphidicolin and hydoxyurea (ApH), as previously reported[28, 29] in an attempt to uncouple the role of Cdk2 from DNA replication. Neutrophil recruitment to the infected ear (Fig. 4a, b) or tailfin amputation sites (Fig. 4c, d) was significantly reduced by the Cdk2 inhibition, but not by DNA replication inhibition. Cdk2 inhibition did not affected total neutrophil numbers in the fish (Fig. 5e, f). In addition, neutrophil motility, but not directionality, was significantly inhibited by the Cdk2 inhibitor (Fig. 4g-I and Video S2), recapitulating the phenotypes resulted from *miR-199* overexpression. To increase our confidence of the results obtained with pharmacological Cdk2 inhibition, two additional Cdk2 inhibitors[30] were used. A CDK2 selective inhibitor CTV313 and a pan-CDK inhibitor roscovitine also blocked neutrophil motility and recruitment in inflammation models (Supplementary Fig. 4 and Video S2). We then tested whether the neutrophils under investigation had indeed exited the cell cycle. No cell division was observed during wounding or infection (Supplementary Fig. 5a, b and Video S3), suggesting that neutrophil division is a rare event. Additionally, less than 3% of the neutrophils in adult kidney marrow were in the S or G2 phase (Supplementary Fig. 5c-e). Because *cdk2* has not been previously implicated in regulating neutrophil migration, primary human neutrophils were isolated and treated with NU6140. Inhibition of CDK2 significantly reduced chemotaxis toward Interleukin-8 (IL-8), with a decreased velocity and chemotaxis index (Fig. 4j-l and Video S4). In summary, we report a previously unknown role for *cdk2* in regulating neutrophil chemotaxis in a way separable from its function in DNA replication.

Catalytic activity of Cdk2 is required for neutrophil motility

We further tested our hypothesis that the kinase activity of Cdk2 is essential for neutrophil motility. We cloned the zebrafish *cdk2* gene and tagged it at the N-terminus with mCherry linked via a self-cleavable 2a peptide (Fig. 5a). Mutations at D145, a residue that chelates Mg^{+2} and facilitates ATP binding to the catalytic cleft [31], resulted in a catalytic-dead and dominant-negative form of Cdk2. We constructed zebrafish lines overexpressing *cdk2* (D145N) in neutrophils, *Tg(lyzC:mcherry-2a-cdk2-d145n)*^{pu19}, together with a control line *Tg(lyzC:mcherry-2a-cdk2)*^{pu20}, hereby referred to as cdk2 D145N or the WT line. We observed a significant reduction of neutrophil motility (Fig. 5b-d and Video S5) and recruitment to the tail amputation site (Fig. 5e, f) in the D145N line. To characterize neutrophil chemotaxis to a single chemoattractant, we bathed embryos from the two lines in Leukotriene B4 (LTB4) and quantified neutrophil emigration from the caudal hematopoietic tissue (CHT) to the caudal fin. The percentage of neutrophils migrating outside the CHT and the distance neutrophils traveled in the caudal fin were significantly reduced in the D145N line (Fig. 5g, h, Supplementary Fig. 6a, b and Video S6). In addition, neutrophil motility in the CHT was reduced (Supplementary Fig. 6c, d and Video S7). To visualize neutrophil cell polarity, the cdk2 D145N or the WT lines were crossed with *Tg(mpx:GFP-UtrCH*) which labels stable actin in the trailing edge of migrating neutrophils[32, 33]. In Cdk2 D145N expressing neutrophils, stable actin is enriched in transient cell protrusions that quickly retract in multiple directions, displaying disrupted cell polarity and actin dynamics (Fig.5i and Video S8). Together, our results indicate that the catalytic activity of Cdk2 is required for neutrophil polarization and chemotaxis.

***miR-199* overexpression or Cdk2 inhibition ameliorates systemic inflammation**

With the findings that *miR-199* overexpression or *cdk2* abrogation hinders neutrophil chemotaxis, we sought to determine whether these manipulations could alleviate acute systemic inflammation caused by *P. aeruginosa* infection[34, 35]. We thus administered a lethal dose of *P. aeruginosa* directly into the circulation in zebrafish embryos. Survival of the embryos was significantly improved in the *miR-199* line and the *cdk2* D145N line compared with their respective control lines (Fig. 6a, b). Consistently, NU6140 treatment improved the infection outcome whereas DNA replication inhibitors were detrimental to the infected host (Fig. 6c). Roscovitine, a pan CDK inhibitor[36] currently in phase-II trial for cancer treatment, also displayed a protective effect at 15 μM but was detrimental at 30 μM, possibly resulted from the inhibitory effect on cell proliferation and tissue repair as previously reported in cell culture and *ex vivo* bone marrow isolations[37, 38] (Fig. 6d). To assess further the protective effect of dampening neutrophilic inflammation during systemic inflammation, we utilized a sterile inflammation model of endotoxemia[39]. Neutrophil-specific *miR-199* overexpression or roscovitine treatment reduced host mortality (Fig. 6e, f), indicating a host protective effect of *miR-199* overexpression and Cdk2 inhibition during acute systemic inflammation and infection, without generating broad immune suppression.

Discussion

microRNAs play a pivotal role in diseases driven by neutrophilic inflammation[40, 41, 42] where both protective and detrimental effects have been noted. Currently, there is no systemic screen to identify miRNAs that can suppress neutrophil migration, possibly because neutrophils are terminally differentiated and not genetically tractable in cell culture. A microRNA overexpression screen was performed in B cells[13], but not in other immune cells. In the present study, we performed an *in vivo* functional screen in the zebrafish and identified *miR-199* as a critical evolutionarily conserved regulator of neutrophil migration and chemotaxis. *miR-199* hindered neutrophil motility by downregulating genes in the canonical cell cycle pathways, and by directly targeting Cdk2. We further showed that the catalytic activity of Cdk2 was critical for neutrophil migration and chemotaxis, whereas an active cell cycle and DNA replication were not essential (Supplementary Fig. 6e).

Whereas no previous studies have investigated the role of *miR-199* in neutrophils, its role in suppressing inflammation and cell migration has been reported in cancer cells. In ovarian cancer cells, *miR-199* inhibits canonical NF-κB signaling by targeting *ikbkb*, thus preventing the production of pro-inflammatory cytokines[25]. In our current work, the *miR-199-ikbkb* axis was also validated in neutrophils, further supporting the evolutionary conservation of miRNA-target interaction in vertebrates. Suppression of *ikbkb* may also contribute to the survival of zebrafish during systemic inflammatory challenge due to its central role in inflammation. From the perspective of cell migration, *miR-199* hinders cancer cell migration and invasion by downregulating β1 integrin levels[43], decreasing CD44 and interaction with Ezrin[44], or by directly targeting α3 integrin[45] in various cancer cells. Low levels of *miR-199* correlate with poor prognosis, increased cell proliferation and metastasis. Subsequent introduction of *miR-199* alleviated invasiveness *in vitro* through targeting the Wnt or HIF-1α/VEGF pathways[46, 47]. Here we provide evidence that *miR-199* is a suppressor of cell migration in leukocytes, expanding its role to inflammation. Our observation is in line with a recent report that *miR-199a-5p* is increased in the plasma in patients with neutrophilic asthma[48] and inflammatory bowel disease[49], suggesting that miR-199 may play physiological functions in inflammation. In addition, *miR-*

199b suppress myeloid differentiation[50], which can also contribute to its role in suppressing the innate immunity.

The most surprising finding of our study is that *miR-199* predominantly regulates the cell cycle-dependent kinase *CDK2* in terminally differentiated neutrophils that have exited the cell cycle. The function of CDK2 has not previously been investigated in the context of inflammation. CDK2 is a cell cycle-dependent kinase whose cofactors, cyclin E and A, are expressed during mitosis, activating its kinase activity and cell cycle progression[51]. CDK2 is a facilitator of the cell cycle during G1/S phase (with cyclin E) and S/G2 phase (with cyclin A)[52], and deletion of CDK2 prolongs but does not inhibit cell cycle progression[53]. CDK2 is required for meiosis during mammalian gametogenesis. In addition, CDK2 phosphorylates transcriptional factors to drive cell cycle progression and cell differentiation, and to alter cell metabolism and DNA double-strand break repair[54].

We provided evidence that the kinase activity of CDK2 is required for neutrophil migration. The limitation of our work is that the direct phosphorylated substrate of CDK2 in neutrophils are not identified, which presents a significant challenge. CDK2 is a serine/threonine protein kinase, which uses the KLAD*FGLA kinase consensus domain to phosphorylate the "Ser/Thr-Pro-X-basicAA" motif of target proteins, although noncanonical target motifs are prevalent[55]. Over a hundred proteins are likely phosphorylated by CDK2-cyclinA in HEK cells[56] and the CDK2-cyclinE substrates are not all characterized. Thus extensive work will be required to characterize how CDK2 contributes to the signaling network required for neutrophil chemotaxis and identify the proteins that are phosphorylated by CDK2 in neutrophils. CDK2 is present in the neutrophil cytosol and its expression is upregulated upon LPS stimulation[57], supporting the possibility that CDK2 ties in the signaling pathways downstream of the immune receptors in neutrophils. As a step closer to the potential mechanism, we have visualized the actin dynamics and the cell polarity in neutrophils with the dominant-negative Cdk2 overexpression. Indeed, stable actin is enriched in the transient protrusions that quickly retract, a phenotype resembling the over expression of a dominant negative Rac2 construct and after PI3K inhibition[33, 58]. It is likely that Cdk2 regulates the Rac2-PI3K axis, which is essential in cell motility.

Acute neutrophilic over-inflammation is a pressing concern in many diseases pathologies[1] and methods of hindering neutrophil migration and inflammation while preserving immune integrity and highly desired. Our study presents an acute method to dampen neutrophil recruitment by inhibiting Cdk2, which reduced the lethality caused by acute systemic inflammation. The pan-CDK inhibitor roscovitine competes with ATP for the occupation of the kinase active site[59] and is currently in multiple phase II clinical trials to inhibit cystic fibrosis and multiple types of tumors (clinicaltrials.gov). Previous studies in mice have shown that treatment of roscovitine at 10-100 mg/kg for 3-7 days after inflammation induction resulted in decreased neutrophil infiltration into the inflamed tissue and better clinical outcome[60]. This reduced neutrophil recruitment was attributed to CDK9 inhibition and neutrophil apoptosis [61] and a direct link to CDK2 was not shown. *Cdk2* knockout mice show normal myeloid cell numbers during resting and stressed conditions[62] and no developmental defects besides having a smaller body size and sterility[63]. Thus CDK2 inhibition is not expected to cause adverse side effect and thus present an attractive strategy for short-term and long-term control of inflammation. Inhibition of CDK2 has been extensive studied in cancers to inhibit cancer cell proliferation[64] but to our knowledge the effect of cdk2 inhibition in neutrophil function or inflammation has not been characterized. Our results here provide a mechanistic understanding of the neutrophil inhibitory effect of roscovitine

and suggest a future direction of utilizing Cdk2 specific inhibitors in managing inflammation, which may be better tolerated than a pan-Cdk inhibitor such as roscovitine.

In summary, our present study demonstrates previously unappreciated roles of *miR-199* and CDK2 in regulating neutrophil migration and points to new directions in managing neutrophilic inflammation.

Materials and Methods:

microRNA seq

Neutrophil and apical epithelial cells were sorted from transgenic zebrafish lines *Tg(lyzC:GFP)* and *Tg(Krt4:GFP*) at 3 day post fertilization (dpf) using fluorescence-activated cell sorting. Total RNA was exacted using Ambion mirVana kit (without enrichment for small RNA). Library was prepared using TruSeq Small RNA Preparation (illumina). After library construction, DNA of 145-160 bp were excited from Invitrogen 6% Novex TBE Gel and sequenced using Illumina HiSeq2000 with paired-end reads of 50 bp with a total of 2-3M/sample. MicroRNA sequence is performed at University of Wisconsin Collaborative Genomics Core. For analysis, sequencing reads were map to the zebrafish genome (GRCz11) using RNA-seq aligner from STAR (v2.5)[65] with the parameter: "--alignEndsType EndToEnd --outFilterMismatchNmax 1 --outFilterMultimapScoreRange 0 --outFilterMultimapNmax 10 --outSAMunmapped Within --outFilterScoreMinOverLread 0 --outFilterMatchNminOverLread 0 --outFilterMatchNmin 16 --alignSJDBoverhangMin 1000". FeatureCounts (from subread v1.5.1)[66] was used to evaluate expression levels of zebrafish mature microRNAs based on uniquely mapped reads with the parameters: "-s 1 –Q 10". Before TMM normalization and DE analysis by edgeR (v3.20.8)[67], microRNAs whose CPM was less than 10 were removed from all samples. Differentially expressed microRNAs were selected if their FDR-adjusted p-values were less than 0.05.

RNA seq

Kidney marrow was dissected from 2 adults from *Tg(lyzC:Dendra2-miR-199-3)*^{pu19} or *Tg(lyzC:Dendra2-vector)*^{pu7} and neutrophils were sorted using fluorescence-activated cell sorting. Total RNA was extracted using RNeasy Plus Mini Kit (Qiagen #74104). RNAseq was performed at The Center for Medical Genomics at Indiana University School of Medicine. Samples were polyA enriched and sequenced with Illumina HiSeq 4000 ultra low with reads range from 37M to 44M. The RNA-seq aligner from the STAR (v2.5)[65] were employed to map RNA-seq reads to the reference genome, zebrafish (GRCz11), with the following parameter: "--outSAMmapqUnique 60". Uniquely mapped sequencing reads were assigned to genes using featureCounts (from subread v1.5.1)[68] with the following parameters: "-p -Q 10". The genes were filtered for further analysis if their count per million (CPM) of reads was less than 0.5 in more than 3 samples. The method of trimmed mean of M values (TMM) was adopted for gene expression normalization cross all samples, followed by differential expression analysis between different conditions using edgeR (v3.20.8). Differentially expressed gene was determined for the comparison if its false discovery rate (FDR) adjusted p-value was less than 0.05 and the amplitude of fold change (FC) was larger than linear 2-fold. The functional analysis was performed on DEGs of our interest with a cutoff of FDR < 0.05 to identify significantly over-represented Gene Ontology (GO) and/or KEGG pathways by using the DAVID[69].

Quantitative RT-PCR:

Total RNA was purified using MiRVANA miRNA purification kit (ThermoFisher). MicroRNAs were reverse transcribed with Universal cDNA Synthesis Kit II (Exiqon). MicroRNA RT-qPCR was performed with ExiLENT SYBR® Green master mix (Exiqon) using LightCycler ® 96 Real-Time PCR System (Roche Life Science). Messenger RNAs were reverse transcribed with Transcriptor First Strand cDNA Synthesis Kit (Roche). RT-qPCR were performed with FastStart Essential DNA Green Master (Roche). The specificity of the primers were verified with a single peak in the melt-curve. The relative fold change with correction of the primer efficiencies was calculated following instructions provided by Real-time PCR Miner (http://ewindup.info/miner/data_submit.htm) and normalized to *U6*. miRNA Primers used in this study are: dre-miR-222b (2111861), dre-miR-146b (2117034), dre-miR-142 (2104518), dre-miR-146a (2114679), dre-miR-21 (2101053), dre-miR-430 (2105859), dre-miR-92a (204258), dre-miR-181a (2100735), dre-miR-31 (2103532), dre-miR-375 (2109706), dre-miR-199-3 (204536), dre-miR-223 (205986), dre-let7e (2106780), dre-U6 (206999), hsa-miR-199 (204536), hsa-miR-100 (205689), hsa-miR-223 (205986), hsa-let7e (205711), hsa-U6 (203907).For One-step RT-qPCR of sorted neutrophils, RNA was extracted as using RNeasy Plus Mini Kit (Qiagen #74104) and one-step RT-qPCR was performed with SuperScript® III Platinum® SYBR® Green One-Step qRT-PCR Kit (Invitrogen), using LightCycler® 96 Real-Time PCR System (Roche Life Science). The relative fold change with correction of the primer efficiencies was calculated following instructions provided by Real-time PCR Miner and normalized to *rpl32*. Primers: dre-cdk1+: 5'-ttggggtcccagtaagagtcta-3'; dre-cdk1-: 5'-ggtgtggaatagcgtgaagc-3'; dre-cdk2+: 5'-agatggcagagaccttctcg-3'; dre-cdk2-: 5'-cggaaaaaccgatgaacaag-3' ; dre-cdk5+: 5'-tgggaacgccaacagaag-3'; dre-cdk5-: 5'- agctggatacatcgggtacg-3' ; dre-cdca8+: 5'-atggcaccgctgaagtctac-3'; dre-cdca8-: 5'-cgttgaaggagctttctttga-3' ; dre-kif14+: 5'-aggaggctcgcttgaagg-3'; dre-kif14-: 5'-ctctttagccacctgaatgc-3' ; dre-mcm5+: 5'-aagctattgcctgcctgct-3'; dre-mcm5-: 5'-ccctcttcgtgtcagaccat-3' ; dre-casp3b+: 5'-caggatattacgcatggagga-3'; dre-casp3b-: 5'- tcgcacagcgaggagataa-3' ; dre-ikbkb+: 5'-gaggagcgagaaacaactgc-3'; dre-ikbkb-: 5'-tggactgcgaactttactgc-3' ; dre-rpl32+: 5'-tcagtctgaccgctatgtcaa-3'; dre-rpl32-: 5'- tgcgcactctgttgtcaatac-3'.

Generation of transgenic zebrafish lines

The zebrafish experiment was conducted in accordance with internationally accepted standards. The Animal Care and Use Protocol was approved by The Purdue Animal Care and Use Committee (PACUC), adhering to the Guidelines for Use of Zebrafish in the NIH Intramural Research Program (protocol number: 1401001018). 300-600bp genomic DNA fragments flanking the respective miRNA were PCR amplified from zebrafish genomic DNA using specific primers and inserted into the *Bbs*I site in the vector backbone as described[20]. Zebrafish *cdk2* gene was cloned from zebrafish mRNA using SuperScript III RT-kit (Invitrogen #18080044) and amplified with the following primers. zCdk2+: 5′-GAAAACCCCGGTCCTATGGAGTCTTTTCAGAAAGTGGAG-3′; zCdk2-: 5′-CATGGCTGATTATGATTATAGGCGTAAAGGAGGCACTGG-3′ and inserted into a Tol2-mcherry-2A backbone. Point mutation was generated using infusion (Takara #638920) site directed mutagenesis with zCdk2 DN+: 5′- ACTGGCTAACTTTGGTTTGGCCAGAGCGTTC -3′; zCdk2 DN -: 5′- CCAAAGTTAGCCAGTTTGATCTCGCCCTG -3′. The plasmids were injected into zebrafish embryo at 1-cell stage and the stable line were generated as previously described[33]. At least two founders (F0) for each *line* were obtained. Experiments were performed using F2 larvae produced by F1 fish derived from multiple founder to minimize the artifacts associated with random insertion sites.

Dual luciferase reporter assay:
Both zebrafish and human *CDK2* 3′UTR were amplified from zebrafish genomic DNA with SuperScript III RT-kit (Invitrogen #18080044) and cloned into psiCHECK2 (Promega) at *Xho*I and *Not*I cloning sites with the following primers: zCDK2+: 5′-TAGGCGATCGCTCGAGAACGAGATCAACTTTGGCAAG-3′; zCdk2-: 5′-TTGCGGCCAGCGGCCGCTGTAACAACATAAACCAAATGTT-3′, hCDK2+: 5′-TAGGCGATCGCTCGAGAGCCTTCTTGAAGCCCCCA-3′; hCdk2-: 5′-TTGCGGCCAGCGGCCGCTATAAAACTAGGCACATTTTTTTAA-3′. Mutated 3′UTR constructs were generated using Infusion HD cloning kit (Clontech) with the following primers: zCdk2 mut+: 5′- CCTGTGTGACCCAAAAAAACAGCTGTGCTAATAGT-3′; zCdk2 mut-: 5′-TTTGGGTCACACAGGTTGCAATGGATAATCTTCA-3′, hCdk2 mut+: 5′-AAAACGTGACCGAGGAGTCTATTTTAAAGAATTCGG. DNA encoding miR-199 or vector were amplified from the construct used for expression in zebrafish and inserted into pcDNA3.1 at the *Hin*dIII/*Xba*I cloning sites using the following primers: pcDNA-199+: 5′-GTTTAAACTTAAGCTTGCCACCATGGATGAGGAAATCGC-3′; pcDNA-199-: 5′-AAACGGGCCCTCTAGAGACCGGTACCCCCGGGCTGC-3′.

Live imaging:
Larvae at 3 dpf were settled on a glass-bottom dish and imaging was performed at 28.5 ºC. Time-lapse fluorescence images in the head mesenchyme were acquired with a laser-scanning confocal microscope (LSM710, Zeiss) with a Plan-Apochromat 20×/0.8 M27 objective. Neutrophil motility at the caudal hematopoietic tissue was imaged using Zeiss EC Plan-NEOFLUAR 10X/0.3 objective. For neutrophil nucleus and cytosol reporter line imaging, a LD C-Apochromat 40x/1.1 W Korr M27 was used. The green and red channels were acquired sequentially with 0.1~0.3% power of the 488 nm laser and 0.5%~2% of 561 nm laser, respectively, with a 200 µm pinhole at a speed of 1.27 µs/pixel and averaged (line 2). The fluorescent stacks were flattened using the maximum intensity projection and overlaid with a single slice of the bright-field image. Neutrophil chemotaxis upon LTB4 treatment was captured with a Zeiss ZV16 dissection microscope at 2x magnification every 15sec for 30 minutes.

Inflammation assays in zebrafish:
Zebrafish wounding and infection were performed as described[20]. For LTB4 recruitment assays, 3 dpf zebrafish larvae were treated with 30 nM LTB4 for 15 minutes and fixed. Neutrophils were stained with Sudan Black and the number at the indicated regions were quantified.

Generation of stable HL-60 cell lines:
HEK-293 cells were cultured in DMEM supplemented with 10% FBS, 4.5 g/glucose and sodium bicarbonate. HL-60 cells were obtained from ATCC (CCL-240) and cultured using RPMI-1640 with HEPES supplemented with 10% FBS and sodium bicarbonate. The lentiviral backbone pLIX_403 was a gift from David Root (Addgene plasmid # 41395). The DNA sequence flanking *MIR-199* was cloned from HL-60 cell genomic DNA and cloned into a backbone containing Dendra2. The miRNA and dendra2 reporter were then cloned into pLIX_403 vector using the NheI/AgeI sites with primer set: pLIX-mir+: 5’ TGGAGAATTGGCTAGCGCCACCATGGATGAGGAAA TCGC-3’, pLIX-mir-: 5’-CATACGGATAACCGGTTACCACACCTGGCTGGGC-3’. Stable HL-60 cell lines were generated as described.[70] Briefly, HEK-293 cells were transfected with pLIX_403, VSV-G and CMV8.2 using lipofectamine 3000 (ThermoFisher). The viral supernatant was harvested on day three and concentrated with Lenti-X concentrator (Clontech).

HL-60 Cells were infected at 2000 g for 2 h at 32 ºC and maintained in medium supplemented with 1 µg/ml puromycin. Live cells that excluded trypan blue were counted using a hemocytometer.

Flow Cytometry:
Cells were stained with Alexa Fluor 647 conjugated CD11b (neutrophil differentiation marker, Biolegend, 301319, clone IV-M047, 2ul to $1X10^6$ cells) or the isotype control antibody (Biolegend, 400130, clone MOPC-21, 2ul to $1X10^6$ cells) and RUO AnnexinV (apoptosis marker, BD, 563973, 5ul to $1X10^6$ cells). Cells were stained in staining buffer (1% BSA, 0.1% NaN3) and incubated on ice for 1 hour, washed three times with staining buffer and resuspended in suitable volumes. Cell cycle profiling was obtained using Vybrant™ DyeCycle™ Ruby Stain (Thermo #V10309) following the manufacture's protocol. Fluorescence intensity were collected using BD LSR Fortessa. Results were analyzed with Beckman Kaluza 2.1 software.

Inhibitor treatment for zebrafish larvae:
CDK2 inhibitors NU6140 (Enzo # ALX-270-441), CTV313 (Sigma #238803) and roscovitine (Selleckchem #S1153) were dissolved in DMSO to make a 100 mM stock, then further diluted in E3 to working concentrations (100 µM for recruitment and motility assays, and indicated concentration for survival assays). For inhibiting DNA replication, 150 µM aphidicolin and 20 mM hydroxyurea (Sigma #A0781) in 1% DMSO was used as previously described[28, 71]. For neutrophil recruitment and random motility assays, larval were pretreated with the inhibitor for 1 h before experimental procedures. For survival assays, larval were pretreated and kept in the inhibitors from1 hour post infection.

Primary neutrophil isolation and chemotaxis assay:
Primary human neutrophils were isolated with Milteny MACSxpress Neutrophil Isolation Kit. Cells were stain for 10 min with Calcein AM and washed with PBS. 10 million cells/ml were incubated in RPMI+0.1% HSA containing 50 µM NU6104 or DMSO at 37ºC/5% CO_2 for 45 min. Microfluidic devices were fabricated as previously described[72]. Microfluidic chambers were coated with 10 µg/ml fibrinogen for 1 h at 37 °C in PBS. 3 µl of neutrophil suspension (4×10^6 cells/ml) was added to the device, and 5 µM IL-8 was added to the source port. The gradient was allowed to set up and equilibrate in a 37 °C humidified chamber for 15 min before imaging. Time-lapse imaging was performed using a 10×, NA of 0.45, or 60×, NA of 1.4 objective and motorized stage (Ludl Electronic Products) on an inverted microscope (Eclipse TE300) using a charge-coupled device camera (CoolSNAP ES2) and captured into MetaVue imaging software v6.2. Images were taken every 30 s for 30–45 min with up to eight devices being imaged simultaneously. Tracking and velocity quantification were performed as described[7].

Statistical Analysis:
Statistical analysis was carried out using PRISM 6 (GraphPad). Mann–Whitney test (comparing two groups), Kruskal–Wallis test (when comparing to single group), and Gehan–Breslow–Wilcoxon test (for survival curve comparison) were used in this study as indicated in the figure legends. Individual p values are indicated in the figure with no data points excluded from statistical analysis. One representative experiment of at least three independent repeats are shown. For qPCR, each gene was normalized to a reference gene and compared with Holm-Sidak test

(individual comparison with paired value) where each p value and DF was adjusted for respective multiple comparisons.

Data Availability:
The microRNA-seq and RNA-seq raw and processed data are submitted to the Gene Expression Omnibus (GSE127174). Plasmids are available on Addgene.

References:

1. Sadik CD, Kim ND, Luster AD. Neutrophils cascading their way to inflammation. *Trends Immunol* 2011, **32**(10)**:** 452-460.
2. Nathan C. Neutrophils and immunity: challenges and opportunities. *Nature reviews Immunology* 2006, **6**(3)**:** 173-182.
3. Soehnlein O, Steffens S, Hidalgo A, Weber C. Neutrophils as protagonists and targets in chronic inflammation. *Nature Reviews Immunology* 2017, **17**(4)**:** 248-261.
4. Sonego F, Castanheira FV, Ferreira RG, Kanashiro A, Leite CA, Nascimento DC, *et al.* Paradoxical Roles of the Neutrophil in Sepsis: Protective and Deleterious. *Frontiers in immunology* 2016, **7:** 155.
5. Mocsai A, Walzog B, Lowell CA. Intracellular signalling during neutrophil recruitment. *Cardiovascular research* 2015, **107**(3)**:** 373-385.
6. Lammermann T, Bader BL, Monkley SJ, Worbs T, Wedlich-Soldner R, Hirsch K, *et al.* Rapid leukocyte migration by integrin-independent flowing and squeezing. *Nature* 2008, **453**(7191)**:** 51-55.
7. Yamahashi Y, Cavnar PJ, Hind LE, Berthier E, Bennin DA, Beebe D, *et al.* Integrin associated proteins differentially regulate neutrophil polarity and directed migration in 2D and 3D. *Biomedical microdevices* 2015, **17**(5)**:** 100.
8. Friedman RC, Farh KKH, Burge CB, Bartel DP. Most mammalian mRNAs are conserved targets of microRNAs. *Genome Res* 2009, **19**(1)**:** 92-105.
9. Gurol T, Zhou W, Deng Q. MicroRNAs in neutrophils: potential next generation therapeutics for inflammatory ailments. *Immunological reviews* 2016, **273**(1)**:** 29-47.
10. Rupaimoole R, Slack FJ. MicroRNA therapeutics: towards a new era for the management of cancer and other diseases. *Nature Reviews Drug Discovery* 2017, **16**(3)**:** 203-221.
11. Olarerin-George AO, Anton L, Hwang YC, Elovitz MA, Hogenesch JB. A functional genomics screen for microRNA regulators of NF-kappaB signaling. *BMC biology* 2013, **11:** 19.
12. Kim K, Vinayagam A, Perrimon N. A Rapid Genome-wide MicroRNA Screen Identifies miR-14 as a Modulator of Hedgehog Signaling. *Cell reports* 2014, **7**(6)**:** 2066-2077.
13. Gonzalez-Martin A, Adams BD, Lai M, Shepherd J, Salvador-Bernaldez M, Salvador JM, *et al.* The microRNA miR-148a functions as a critical regulator of B cell tolerance and autoimmunity. *Nature immunology* 2016, **17**(4)**:** 433-440.
14. Johnnidis JB, Harris MH, Wheeler RT, Stehling-Sun S, Lam MH, Kirak O, *et al.* Regulation of progenitor cell proliferation and granulocyte function by microRNA-223. *Nature* 2008, **451**(7182)**:** 1125-1129.
15. Fan HB, Liu YJ, Wang L, Du TT, Dong M, Gao L, *et al*. miR-142-3p acts as an essential modulator of neutrophil development in zebrafish. *Blood* 2014, **124**(8)**:** 1320-1330.

16. Zhou WQ, Pal AS, Hsu AYH, Gurol T, Zhu XG, Wirbisky-Hershberger SE, *et al.* MicroRNA-223 Suppresses the Canonical NF-kappa B Pathway in Basal Keratinocytes to Dampen Neutrophilic Inflammation. *Cell reports* 2018, **22**(7)**:** 1810-1823.
17. Sullivan C, Kim CH. Zebrafish as a model for infectious disease and immune function. *Fish & shellfish immunology* 2008, **25**(4)**:** 341-350.
18. Lieschke GJ, Currie PD. Animal models of human disease: zebrafish swim into view. *Nature reviews Genetics* 2007, **8**(5)**:** 353-367.
19. Takaki K, Cosma CL, Troll MA, Ramakrishnan L. An in vivo platform for rapid high-throughput antitubercular drug discovery. *Cell reports* 2012, **2**(1)**:** 175-184.
20. Hsu AY, Wang DC, Gurol T, Zhou WQ, Zhu XG, Lu HY, *et al.* Overexpression of microRNA-722 fine-tunes neutrophilic inflammation by inhibiting Rac2 in zebrafish. *Disease models & mechanisms* 2017, **10**(11)**:** 1323-1332.
21. Taganov KD, Boldin MP, Chang KJ, Baltimore D. NF-kappa B-dependent induction of microRNA miR-146, an inhibitor targeted to signaling proteins of innate immune responses. *Proceedings of the National Academy of Sciences of the United States of America* 2006, **103**(33)**:** 12481-12486.
22. Jacob C, Leport M, Szilagyi C, Allen JM, Berttand C, Lagente V. DMSO-treated HL60 cells: a model of neutrophil-like cells mainly expressing PDE4B subtype. *International immunopharmacology* 2002, **2**(12)**:** 1647-1656.
23. He L, Hannon GJ. Micrornas: Small RNAs with a big role in gene regulation. *Nature Reviews Genetics* 2004, **5**(7)**:** 522-531.
24. Lahoz-Beneytez J, Elemans M, Zhang Y, Ahmed R, Salam A, Block M, *et al.* Human neutrophil kinetics: modeling of stable isotope labeling data supports short blood neutrophil half-lives. *Blood* 2016, **127**(26)**:** 3431-3438.
25. Chen R, Alvero AB, Silasi DA, Kelly MG, Fest S, Visintin I, *et al.* Regulation of IKK beta by miR-199a affects NF-kappa B activity in ovarian cancer cells. *Oncogene* 2008, **27**(34)**:** 4712-4723.
26. Rossi AG, Sawatzky DA, Walker A, Ward C, Sheldrake TA, Riley NA, *et al.* Cyclin-dependent kinase inhibitors enhance the resolution of inflammation by promoting inflammatory cell apoptosis. *Nature medicine* 2006, **12**(9)**:** 1056-1064.
27. Pennati M, Campbell AJ, Curto M, Binda M, Cheng Y, Wang LZ, *et al.* Potentiation of paclitaxel-induced apoptosis by the novel cyclin-dependent kinase inhibitor NU6140: a possible role for survivin down-regulation. *Molecular cancer therapeutics* 2005, **4**(9)**:** 1328-1337.
28. Zhang LX, Kendrick C, Julich D, Holley SA. Cell cycle progression is required for zebrafish somite morphogenesis but not segmentation clock function. *Development* 2008, **135**(12)**:** 2065-2070.
29. Fukuhara S, Zhang JH, Yuge S, Ando K, Wakayama Y, Sakaue-Sawano A, *et al.* Visualizing the cell-cycle progression of endothelial cells in zebrafish. *Developmental biology* 2014, **393**(1)**:** 10-23.
30. Bhattacharjee RN, Banks GC, Trotter KW, Lee HL, Archer TK. Histone H1 phosphorylation by cdk2 selectively modulates mouse mammary tumor virus transcription through chromatin remodeling. *Molecular and cellular biology* 2001, **21**(16)**:** 5417-5425.
31. Vandenheuvel S, Harlow E. Distinct Roles for Cyclin-Dependent Kinases in Cell-Cycle Control. *Science* 1993, **262**(5142)**:** 2050-2054.

32. Burkel BM, von Dassow G, Bement WM. Versatile fluorescent probes for actin filaments based on the actin-binding domain of utrophin. *Cell motility and the cytoskeleton* 2007, **64**(11)**:** 822-832.
33. Deng Q, Yoo SK, Cavnar PJ, Green JM, Huttenlocher A. Dual Roles for Rac2 in Neutrophil Motility and Active Retention in Zebrafish Hematopoietic Tissue. *Developmental cell* 2011, **21**(4)**:** 735-745.
34. van der Vaart M, van Soest JJ, Spaink HP, Meijer AH. Functional analysis of a zebrafish myd88 mutant identifies key transcriptional components of the innate immune system. *Disease models & mechanisms* 2013, **6**(3)**:** 841-854.
35. Brannon MK, Davis JM, Mathias JR, Hall CJ, Emerson JC, Crosier PS, *et al.* Pseudomonas aeruginosa Type III secretion system interacts with phagocytes to modulate systemic infection of zebrafish embryos. *Cellular microbiology* 2009, **11**(5)**:** 755-768.
36. Bach S, Knockaert M, Reinhardt J, Lozach O, Schmitt S, Baratte B, *et al.* Roscovitine targets, protein kinases and pyridoxal kinase. *The Journal of biological chemistry* 2005, **280**(35)**:** 31208-31219.
37. Song H, Vita M, Sallam H, Tehranchi R, Nilsson C, Siden A, *et al.* Effect of the Cdk-inhibitor roscovitine on mouse hematopoietic progenitors in vivo and in vitro. *Cancer Chemother Pharmacol* 2007, **60**(6)**:** 841-849.
38. Cui CY, Wang YN, Wang YJ, Zhao M, Peng SQ. Exploring the Relationship between the Inhibition Selectivity and the Apoptosis of Roscovitine-Treated Cancer Cells. *J Anal Methods Chem* 2013.
39. Hsu AY, Gurol T, Sobreira TJP, Zhang S, Moore N, Cai CF, *et al.* Development and Characterization of an Endotoxemia Model in Zebra Fish. *Frontiers in immunology* 2018, **9**.
40. Cao MW, Shikama Y, Anzai M, Kimura J. Impaired Neutrophil Migration Resulting from Mir-34a and Mir-155 Overexpressed in Neutrophils from Myelodysplastic Syndrome Patients. *Blood* 2015, **126**(23).
41. Surmiak M, Hubalewska-Mazgaj M, Wawrzycka-Adamczyk K, Musia J, Sanak M. Neutrophil MiRNA-128-3p is Decreased During Active Phase of Granulomatosis with Polyangiitis. *Curr Genomics* 2015, **16**(5)**:** 359-365.
42. Arroyo AB, de los Reyes-Garcia AM, Rivera-Caravaca JM, Valledor P, Garcia-Barbera N, Roldan V, *et al.* MiR-146a Regulates Neutrophil Extracellular Trap Formation That Predicts Adverse Cardiovascular Events in Patients With Atrial Fibrillation. *Arterioscl Throm Vas* 2018, **38**(4)**:** 892-902.
43. Li WT, Wang H, Zhang JB, Zhai LM, Chen WJ, Zhao CL. miR-199a-5p regulates beta 1 integrin through Ets-1 to suppress invasion in breast cancer. *Cancer science* 2016, **107**(7)**:** 916-923.
44. Wang SH, Zhou JD, He QY, Yin ZQ, Cao K, Luo CQ. MiR-199a inhibits the ability of proliferation and migration by regulating CD44-Ezrin signaling in cutaneous squamous cell carcinoma cells. *Int J Clin Exp Patho* 2014, **7**(10)**:** 7131-7141.
45. Koshizuka K, Hanazawa T, Kikkawa N, Arai T, Okato A, Kurozumi A, *et al.* Regulation of ITGA3 by the anti-tumor miR-199 family inhibits cancer cell migration and invasion in head and neck cancer. *Cancer science* 2017, **108**(8)**:** 1681-1692.
46. Song J, Gao L, Yang G, Tang S, Xie H, Wang Y, *et al.* MiR-199a regulates cell proliferation and survival by targeting FZD7. *PloS one* 2014, **9**(10)**:** e110074.

47. Ye H, Pang L, Wu Q, Zhu Y, Guo C, Deng Y, *et al.* A critical role of mir-199a in the cell biological behaviors of colorectal cancer. *Diagn Pathol* 2015, **10:** 65.
48. Huang Y, Zhang S, Fang X, Qin L, Fan Y, Ding D, *et al.* Plasma miR-199a-5p is increased in neutrophilic phenotype asthma patients and negatively correlated with pulmonary function. *PloS one* 2018, **13**(3)**:** e0193502.
49. Xu XM, Zhang HJ. miRNAs as new molecular insights into inflammatory bowel disease: crucial regulators in autoimmunity and inflammation. *World J Gastroentero* 2016, **22**(7)**:** 2206-2218.
50. Favreau AJ, McGlauflin RE, Duarte CW, Sathyanarayana P. miR-199b, a novel tumor suppressor miRNA in acute myeloid leukemia with prognostic implications. *Exp Hematol Oncol* 2016, **5**.
51. Shenolikar S. PROGRESS IN Molecular Biology and Translational Science Protein Phosphorylation in Health and Disease Preface. *Prog Mol Biol Transl* 2012, **106:** Xv-Xvii.
52. Hydbring P, Malumbres M, Sicinski P. Non-canonical functions of cell cycle cyclins and cyclin-dependent kinases. *Nat Rev Mol Cell Bio* 2016, **17**(5)**:** 280-292.
53. Su TT, Stumpff J. Promiscuity rules? The dispensability of cyclin E and Cdk2. *Science's STKE : signal transduction knowledge environment* 2004, **2004**(224)**:** pe11.
54. Hydbring P, Malumbres M, Sicinski P. Non-canonical functions of cell cycle cyclins and cyclin-dependent kinases. *Nature reviews Molecular cell biology* 2016, **17**(5)**:** 280-292.
55. Higashi H, Suzuki-Takahashi I, Taya Y, Segawa K, Nishimura S, Kitagawa M. Differences in substrate specificity between Cdk2-cyclin A and Cdk2-cyclin E in vitro. *Biochemical and biophysical research communications* 1995, **216**(2)**:** 520-525.
56. Chi Y, Welcker M, Hizli AA, Posakony JJ, Aebersold R, Clurman BE. Identification of CDK2 substrates in human cell lysates. *Genome biology* 2008, **9**(10)**:** R149.
57. Leitch AE, Lucas CD, Marwick JA, Duffin R, Haslett C, Rossi AG. Cyclin-dependent kinases 7 and 9 specifically regulate neutrophil transcription and their inhibition drives apoptosis to promote resolution of inflammation. *Cell Death Differ* 2012, **19**(12)**:** 1950-1961.
58. Yoo SK, Deng Q, Cavnar PJ, Wu YI, Hahn KM, Huttenlocher A. Differential Regulation of Protrusion and Polarity by PI(3)K during Neutrophil Motility in Live Zebrafish. *Developmental cell* 2010, **18**(2)**:** 226-236.
59. Otyepka M, Bartova I, Kriz Z, Koca J. Different mechanisms of CDK5 and CDK2 activation as revealed by CDK5/p25 and CDK2/cyclin A dynamics. *Journal of Biological Chemistry* 2006, **281**(11)**:** 7271-7281.
60. Rossi AG, Sawatzky DA, Walker A, Ward C, Sheldrake TA, Riley NA, *et al.* Cyclin-dependent kinase inhibitors enhance the resolution of inflammation by promoting inflammatory cell apoptosis (vol 12, pg 1056, 2006). *Nature medicine* 2006, **12**(12)**:** 1434-1434.
61. Hoodless LJ, Lucas CD, Duffin R, Denvir MA, Haslett C, Tucker CS, *et al.* Genetic and pharmacological inhibition of CDK9 drives neutrophil apoptosis to resolve inflammation in zebrafish in vivo. *Scientific reports* 2016, **5:** 36980.
62. Jayapal SR, Wang CQ, Bisteau X, Caldez MJ, Lim S, Tergaonkar V, *et al.* Hematopoiesis specific loss of Cdk2 and Cdk4 results in increased erythrocyte size and delayed platelet recovery following stress. *Haematologica* 2015, **100**(4)**:** 434-441.

63. Berthet C, Aleem E, Coppola V, Tessarollo L, Kaldis P. Cdk2 knockout mice are viable. *Current Biology* 2003, **13**(20)**:** 1775-1785.
64. Asghar U, Witkiewicz AK, Turner NC, Knudsen ES. The history and future of targeting cyclin-dependent kinases in cancer therapy. *Nature Reviews Drug Discovery* 2015, **14**(2)**:** 130-146.
65. Dobin A, Davis CA, Schlesinger F, Drenkow J, Zaleski C, Jha S, *et al.* STAR: ultrafast universal RNA-seq aligner. *Bioinformatics* 2013, **29**(1)**:** 15-21.
66. Simopoulos AP. Diagnostic implications of cleft palate in the newborn. *Journal of the American Medical Women's Association* 1966, **21**(11)**:** 921-923.
67. Robinson MD, McCarthy DJ, Smyth GK. edgeR: a Bioconductor package for differential expression analysis of digital gene expression data. *Bioinformatics* 2010, **26**(1)**:** 139-140.
68. Liao Y, Smyth GK, Shi W. featureCounts: an efficient general purpose program for assigning sequence reads to genomic features. *Bioinformatics* 2014, **30**(7)**:** 923-930.
69. Huang da W, Sherman BT, Lempicki RA. Systematic and integrative analysis of large gene lists using DAVID bioinformatics resources. *Nature protocols* 2009, **4**(1)**:** 44-57.

70. Cavnar PJ, Berthier E, Beebe DJ, Huttenlocher A. Hax1 regulates neutrophil adhesion and motility through RhoA. *The Journal of cell biology* 2011, **193**(3)**:** 465-473.
71. Naylor RW, Chang HHG, Qubisi S, Davidson AJ. A novel mechanism of gland formation in zebrafish involving transdifferentiation of renal epithelial cells and live cell extrusion. *Elife* 2018, **7**.
72. Berthier E, Lim FY, Deng Q, Guo CJ, Kontoyiannis DP, Wang CCC, *et al.* Low-Volume Toolbox for the Discovery of Immunosuppressive Fungal Secondary Metabolites. *PLoS pathogens* 2013, **9**(4).

Acknowledgements: The work was supported by research funding from National Institutes of Health [R35GM119787 to DQ], [R35GM119787 to AH] and [P30CA023168 to Purdue Center for Cancer Research] for shared resources. Bioinformatics analysis was conducted by the Collaborative Core for Cancer Bioinformatics (C^3B) shared by the Indiana University Simon Cancer Center [P30CA082709] and the Purdue University Center for Cancer Research with support from the Walther Cancer Foundation. AH is supported by Purdue Research Foundation. Dr. Stanton Gelvin (Purdue University) proofread and provided comments.

Authorship Contributions: AH, JW and DQ designed research and wrote the manuscript. AH, DW, JL, DB performed the experiments. AH, DW, JL, JW, RS, DB and SL analyzed data. All authors read and approved the manuscript.

Competing interests: The authors declare no competing interests.

Materials & Correspondence: Correspondence and material requests should be addressed to Qing Deng (deng67@purdue.edu).

Figure Legends:

Figure 1. Identification of miRNAs that suppress neutrophil recruitment in vivo.

(a) Differentially expressed genes (DEGs) of microRNAs in zebrafish neutrophils compared to whole embryo. (b) Quantification of selected miRs that were differentially expressed in neutrophils. (c) Differentially expressed genes (DEGs) of microRNAs in zebrafish epical keratinocytes compared to whole embryo. (d) Quantification of selected miRs that were differentially expressed in keratinocytes. Assay was done with 3 biological repeats each containing cells sorted from at least 100 larvae/repeat. Result is presented as mean ± SD, Holm-Sidak test. (e) Neutrophil recruitment to infected ear in transgenic lines with neutrophil specific overexpression of individual microRNAs. Results were normalized to number of neutrophils recruited in the vector expressing control lines in each individual experiment. (f) Neutrophil recruitment to tail fin transection sites in transgenic lines as described in c. (g, h) Representative images (g) and quantification (h) of neutrophils recruited to infected ear in vector or *miR-199-3* overexpressing zebrafish line. Scale bar, 100 µm. (i, j) Representative images (i) and quantification (j) of neutrophils recruited to tail fin transection sites in vector or *miR-199-3* overexpressing zebrafish line. Scale bar, 200 µm. (g-j) Assays were done with at least 2 individual founders with 3 biological repeats each containing 20 fish per group. Result is presented as mean ± s.d., Kruskal–Wallis test.

Figure 2. *miR-199-3* overexpression reduces neutrophil migration in zebrafish and human.

(a) Quantification of *miR-199*, *miR-223* and *let-7e* levels in neutrophils sorted from the vector or *miR-199-3* zebrafish lines. Neutrophils were isolated from two adult kidney marrows from two different founders. Result are normalized to *u6* and presented as mean ± s.d., Holm-Sidak test. (b, c) Representative images (b) and quantification (c) of total neutrophils in vector or miR-199-3 zebrafish lines. Scale bar, 500 µm. Assays were done with 3 individual founders with 3 biological repeats each containing 20 fish per group. Result from one representative experiment is shown as mean ± s.d., Mann–Whitney test. (d-f) Representative images (d), velocity (e), and meandering index (f) of neutrophil motility in vector or *miR-199-3* zebrafish lines. Scale bar, 100 µm. 3 embryos each from three different founders were imaged and quantification of neutrophils in one representative video is shown. Kruskal–Wallis test. (g) Quantification of *MIR-100/199*, *MIR-233* and *LET-7E* in HL-60 cell lines with/without induced expression of the vector control or *MIR-100/199*. Result from three independent experiments are normalized to *U6* and presented as mean ± s.d., Holm-Sidak test. (h) Transwell migration of HL-60 cells with/without induced expression of the vector control, *MIR-199* or *MIR-100* toward fMLP. Results are presented as mean ± s.d., from three independent experiments and normalized to vector –DOX +fMLP, Kruskal–Wallis test.

Figure 3. *miR-199-3* overexpression suppresses the expression of *Cdk2* in neutrophils.

(a) Volcano blot of DEGs with significant expression changes in *miR-199* expressing neutrophils. Cyan: down-regulated differentially expressed genes (DEGs); Magenta: up-regulated DEGs. (b) Pathway analysis of genes downregulated by *miR-199* in neutrophils. (c) Quantification of the transcript levels of downregulated genes in neutrophils sorted from the vector or *miR-199-3* zebrafish line (at least 100 embryos per group/repeat). Results from three independent experiments are normalized to *rpl32* and presented as mean ± s.d., Holm-Sidak test. (d) Alignment of mature human and zebrafish *miR-199-5p* sequences. (e) Alignment of *miR-199-5p*

and predicted *miR-199* binding sites in human and zebrafish *CDK2* 3´UTR. (f) Suppression of Renilla luciferase expressing via binding to both zebrafish and human CDK2 3´UTRs by *miR-199*. Results from three independent experiments are normalized to firefly luciferase and presented as mean ± s.d., Kruskal–Wallis test.

Figure 4. Inhibition of CDK2 reduces neutrophil motility and chemotaxis in zebrafish and humans.

(a, b) Representative images (a) and quantification (b) of neutrophils recruited to infected ear in zebrafish larva treated with cdk2 inhibitor (NU6140) or DNA replication inhibitors Aphidicolin +hydoxyurea (ApH). Scale bar, 100 µm. (c, d) Representative images (c) and quantification (d) of neutrophils recruited to tail fin transection sites in zebrafish larva treated with NU6140 or ApH. Scale bar, 200 µm. (e, f) Representative images (e) and quantification (f) of total neutrophil number zebrafish larva treated with NU6140 or ApH. Scale bar: 500 µm. (a-f) Assays were done with 3 individual founders with 3 biological repeats each containing 20 fish per group. Result from one representative experiment is shown as mean ± s.d., Mann–Whitney test. (g-i) Representative images (g), velocity (h), and meandering index (i) of neutrophil motility in zebrafish larvae treated with NU6140 or ApH. Scale bar, 100 µm. 3 embryos each from three different founders were imaged and quantification of neutrophils in one representative video is shown, Kruskal–Wallis test. (j-l) Representative tracks (j), mean velocity (k), and chemotaxis index (l) of primary human neutrophils treated with DMSO or NU6140 (50 µM) migrating towards IL-8. Scale bar, 100 µm. Results representative for 3 separate trials are shown. Result is presented as mean ± s.e.m., Two-way paired Welch's t-test.

Figure 5. Dominant-negative CDK2 suppresses neutrophil motility and chemotaxis.

(a) Schematic of the construct for neutrophil specific expression of CDK2 wild-type (WT) or D145N. (b-d) Representative images (b), velocity (c), and meandering index (d) of neutrophil motility in CDK2 WT or D145N zebrafish line. Scale bar, 100 µm. 3 embryos each from three different founders were imaged and quantification of neutrophils in one representative video is shown, Kruskal–Wallis test. (e, f) Representative images (e) and quantification (f) of neutrophil recruitment to the tailfin transection sites in CDK2 WT or D145N zebrafish line. Scale bar, 200 µm. (g, h) Representative images (g) and quantification (h) of neutrophils migrated to the caudal fin (blue box) normalized to total neutrophils in the trunk (red box) in CDK2 WT or D145N zebrafish line. Scale bar, 200 µm. (i) Simultaneous imaging of utrophin-GFP distribution in neutrophils expressing either WT or D145N Cdk2. Data are representative of more than three separate time-lapse videos. Scale Bar, 50µm. (e-h) Assays were done with 3 individual founders with 3 biological repeats each containing 20 fish per group. Result is presented as mean ± s.d., Mann–Whitney test.

Figure 6. Cdk2 inhibition and *miR-199* overexpression improves zebrafish survival during systemic bacterial infection or sterile inflammation.

(a) Survival of zebrafish larvae after infection of 1000 CFU of *P. aeruginosa* i.v in the vector or *miR-199* zebrafish line. Vector lines were left uninfected or injected with PBS as a control. (b) Survival of zebrafish larvae after infection of 1000 CFU of *P. aeruginosa* i.v in the CDK2 WT or D145N zebrafish line. (c) Survival of zebrafish larvae treated with vehicle, NU6140 (100 µM), ApH (150 µM/20 mM) or left untreated after infection of 1000 CFU of *P. aeruginosa* i.v. (d) Survival of zebrafish larvae treated with indicated dilutions of roscovitine infected with 1000

CFU of *P. aeruginosa* i.v.. (e) Survival of zebrafish larvae after injection of 25 ng LPS i.v. in the vector or *miR-199* zebrafish line. (f) Survival of zebrafish larvae treated with indicated dilutions of roscovitine injected with 25ng LPS i.v.. (a-f) One representative experiment of three independent experiments (n >=20 each group) is shown, Gehan–Breslow–Wilcoxon test.

Figure 1

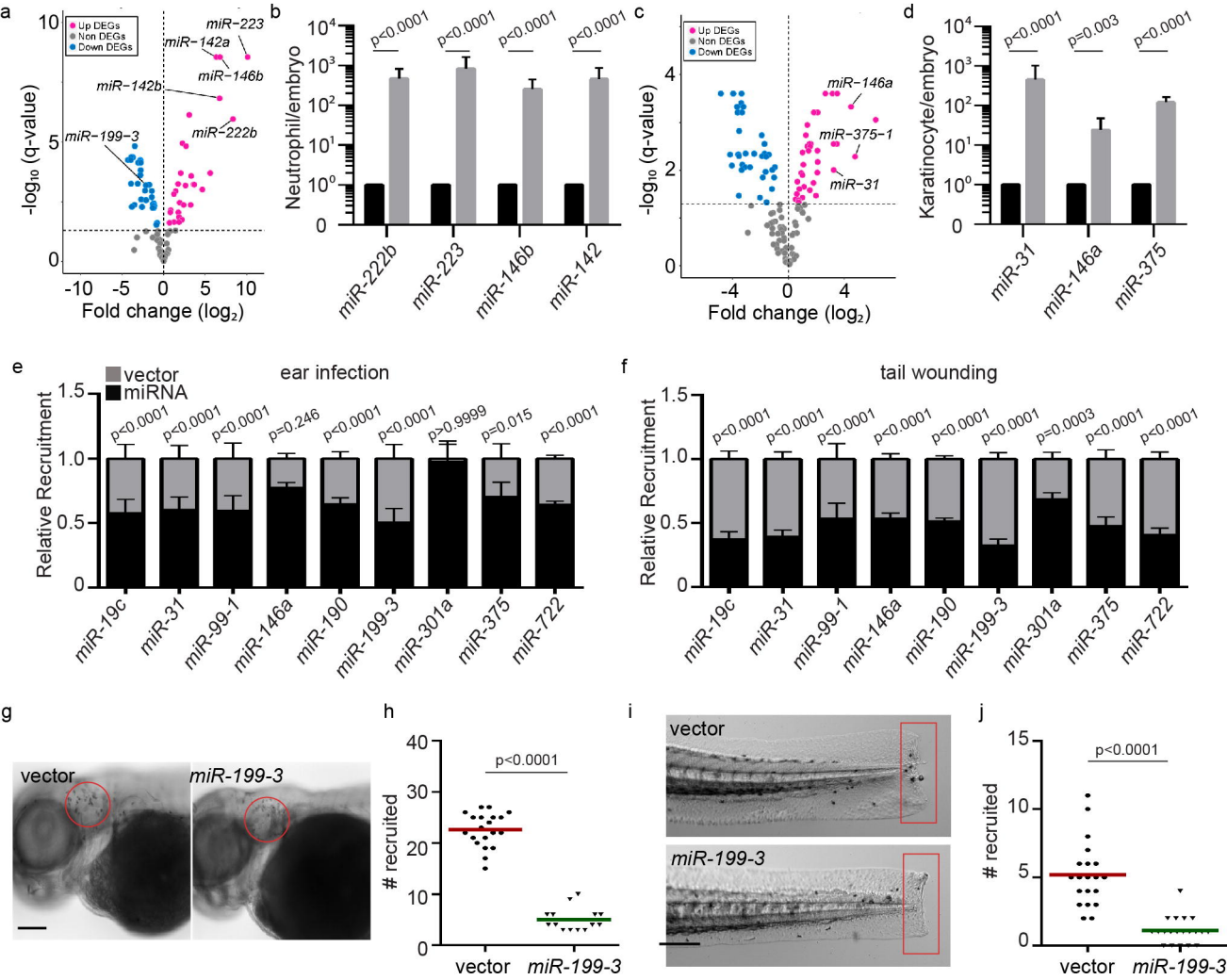
a
Up DEGs
Non DEGs
Down DEGs
miR-223
miR-142a
miR-146b
miR-142b
miR-222b
miR-199-3
-log10 (q-value)
Fold change (log2)
b
Neutrophil/embryo
p<0.0001
miR-222b
miR-223
miR-146b
miR-142
c
Up DEGs
Non DEGs
Down DEGs
miR-146a
miR-375-1
miR-31
-log10 (q-value)
Fold change (log2)
d
Karatinocyte/embryo
p<0.0001
p=0.003
p<0.0001
miR-31
miR-146a
miR-375
e
ear infection
vector
miRNA
Relative Recruitment
p<0.0001
p<0.0001
p<0.0001
p=0.246
p<0.0001
p<0.0001
p>0.9999
p=0.015
p<0.0001
miR-19c
miR-31
miR-99-1
miR-146a
miR-190
miR-199-3
miR-301a
miR-375
miR-722
f
tail wounding
Relative Recruitment
p<0.0001
p<0.0001
p<0.0001
p<0.0001
p<0.0001
p<0.0001
p=0.0003
p<0.0001
p<0.0001
miR-19c
miR-31
miR-99-1
miR-146a
miR-190
miR-199-3
miR-301a
miR-375
miR-722
g
vector
miR-199-3
h
recruited
p<0.0001
vector
miR-199-3
i
vector
miR-199-3
j
recruited
p<0.0001
vector
miR-199-3

Figure 2

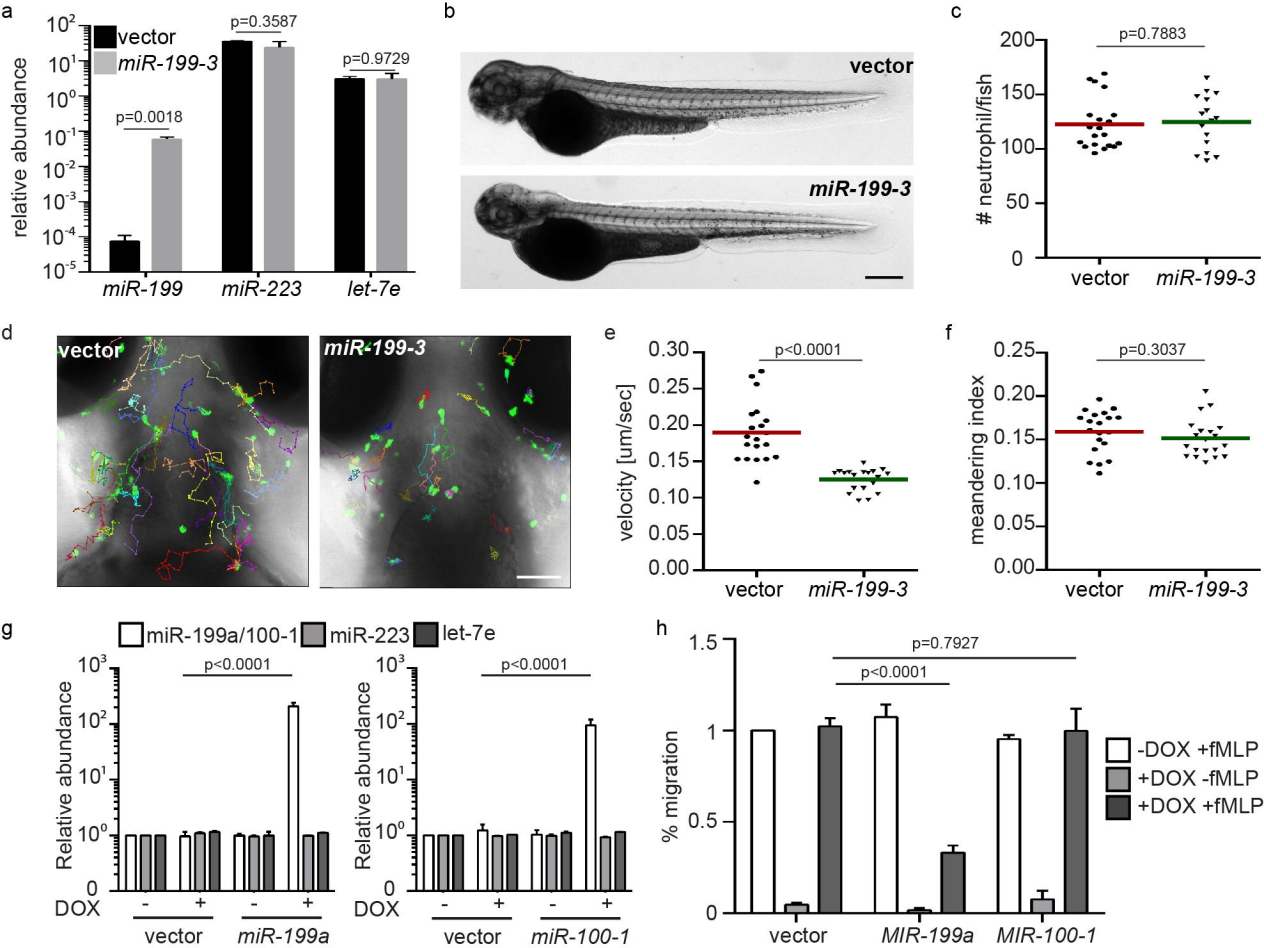
a
vector
miR-199-3
relative abundance
p=0.0018
p=0.3587
p=0.9729
miR-199
miR-223
let-7e
b
vector
miR-199-3
c
p=0.7883
# neutrophil/fish
vector
miR-199-3
d
vector
miR-199-3
e
p<0.0001
velocity [um/sec]
vector
miR-199-3
f
p=0.3037
meandering index
vector
miR-199-3
g
miR-199a/100-1
miR-223
let-7e
p<0.0001
Relative abundance
DOX
vector
miR-199a
p<0.0001
Relative abundance
DOX
vector
miR-100-1
h
p=0.7927
p<0.0001
% migration
-DOX +fMLP
+DOX -fMLP
+DOX +fMLP
vector
MIR-199a
MIR-100-1

Figure 3

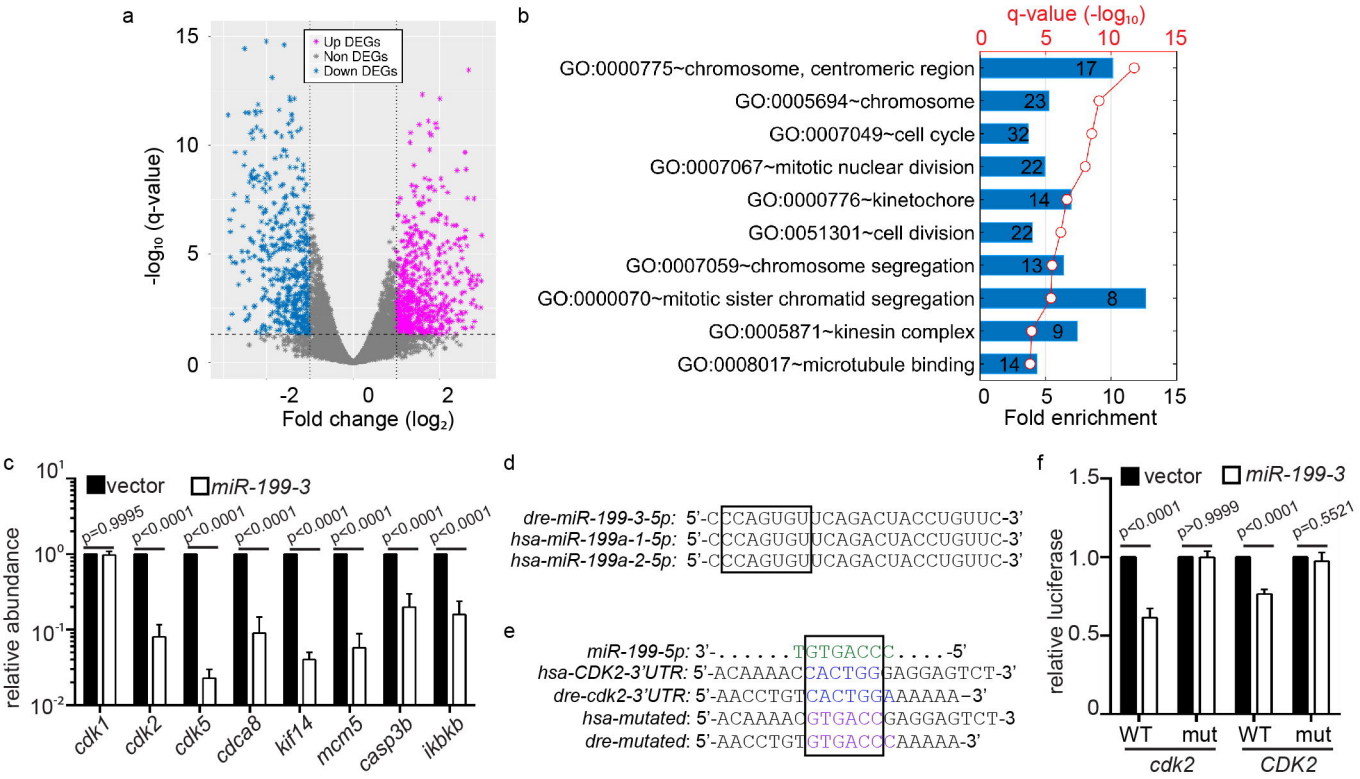
a
Up DEGs
Non DEGs
Down DEGs
-log10 (q-value)
Fold change (log2)
b
q-value (-log10)
GO:0000775~chromosome, centromeric region
GO:0005694~chromosome
GO:0007049~cell cycle
GO:0007067~mitotic nuclear division
GO:0000776~kinetochore
GO:0051301~cell division
GO:0007059~chromosome segregation
GO:0000070~mitotic sister chromatid segregation
GO:0005871~kinesin complex
GO:0008017~microtubule binding
Fold enrichment
c
vector
miR-199-3
relative abundance
p=0.9995
p<0.0001
cdk1
cdk2
cdk5
cdca8
kif14
mcm5
casp3b
ikbkb
d
dre-miR-199-3-5p: 5'-CCCAGUGUUCAGACUACCUGUUC-3'
hsa-miR-199a-1-5p: 5'-CCCAGUGUUCAGACUACCUGUUC-3'
hsa-miR-199a-2-5p: 5'-CCCAGUGUUCAGACUACCUGUUC-3'
e
miR-199-5p: 3'-.....TGTGACCC....-5'
hsa-CDK2-3'UTR: 5'-ACAAAACCACTGGGAGGAGTCT-3'
dre-cdk2-3'UTR: 5'-AACCTGTCACTGGAAAAAA-3'
hsa-mutated: 5'-ACAAAACGTGACCGAGGAGTCT-3
dre-mutated: 5'-AACCTGTGTGACCCAAAAA-3'
f
vector
miR-199-3
relative luciferase
p<0.0001
p>0.9999
p=0.5521
WT
mut
cdk2
CDK2

Figure 4

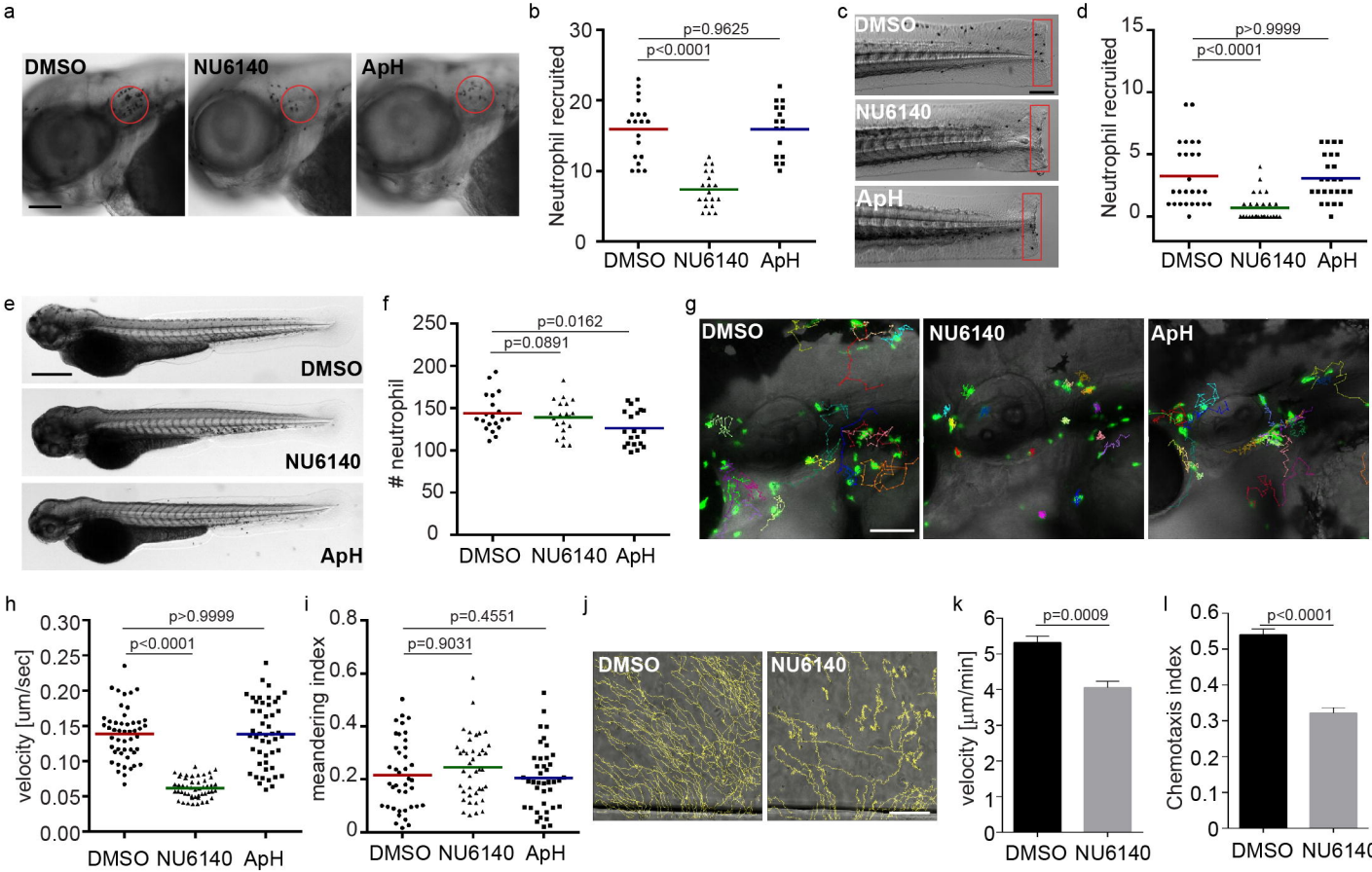
a
DMSO
NU6140
ApH
b
Neutrophil recruited
p=0.9625
p<0.0001
DMSO NU6140 ApH
c
DMSO
NU6140
ApH
d
Neutrophil recruited
p>0.9999
p<0.0001
DMSO NU6140 ApH
e
DMSO
NU6140
ApH
f
# neutrophil
p=0.0162
p=0.0891
DMSO NU6140 ApH
g
DMSO
NU6140
ApH
h
velocity [um/sec]
p>0.9999
p<0.0001
DMSO NU6140 ApH
i
meandering index
p=0.4551
p=0.9031
DMSO NU6140 ApH
j
DMSO
NU6140
k
velocity [µm/min]
p=0.0009
DMSO NU6140
l
Chemotaxis index
p<0.0001
DMSO NU6140

Figure 5

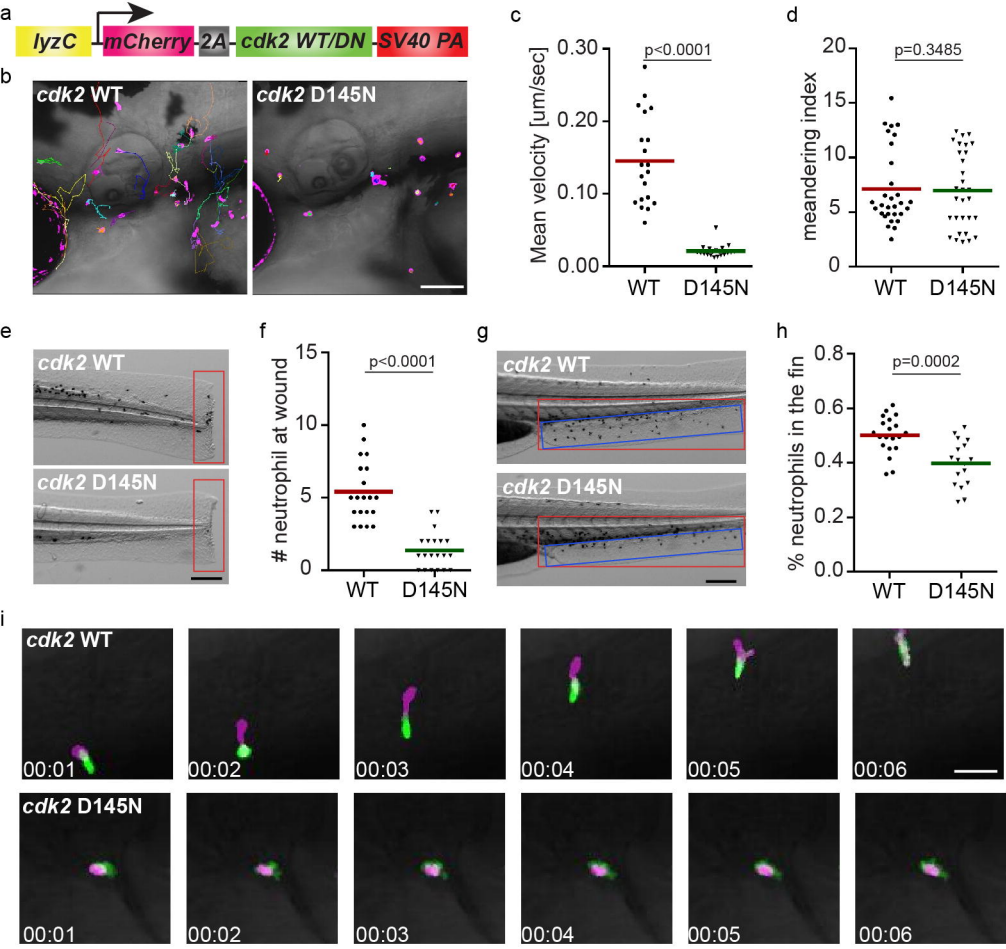
a
lyzC
mCherry
2A
cdk2 WT/DN
SV40 PA
b
cdk2 WT
cdk2 D145N
c
p<0.0001
Mean velocity [um/sec]
0.30
0.20
0.10
0.00
WT
D145N
d
p=0.3485
meandering index
20
15
10
5
0
WT
D145N
e
cdk2 WT
cdk2 D145N
f
p<0.0001
neutrophil at wound
15
10
5
0
WT
D145N
g
cdk2 WT
cdk2 D145N
h
p=0.0002
% neutrophils in the fin
0.8
0.6
0.4
0.2
0.0
WT
D145N
i
cdk2 WT
00:01
00:02
00:03
00:04
00:05
00:06
cdk2 D145N
00:01
00:02
00:03
00:04
00:05
00:06

Figure 6

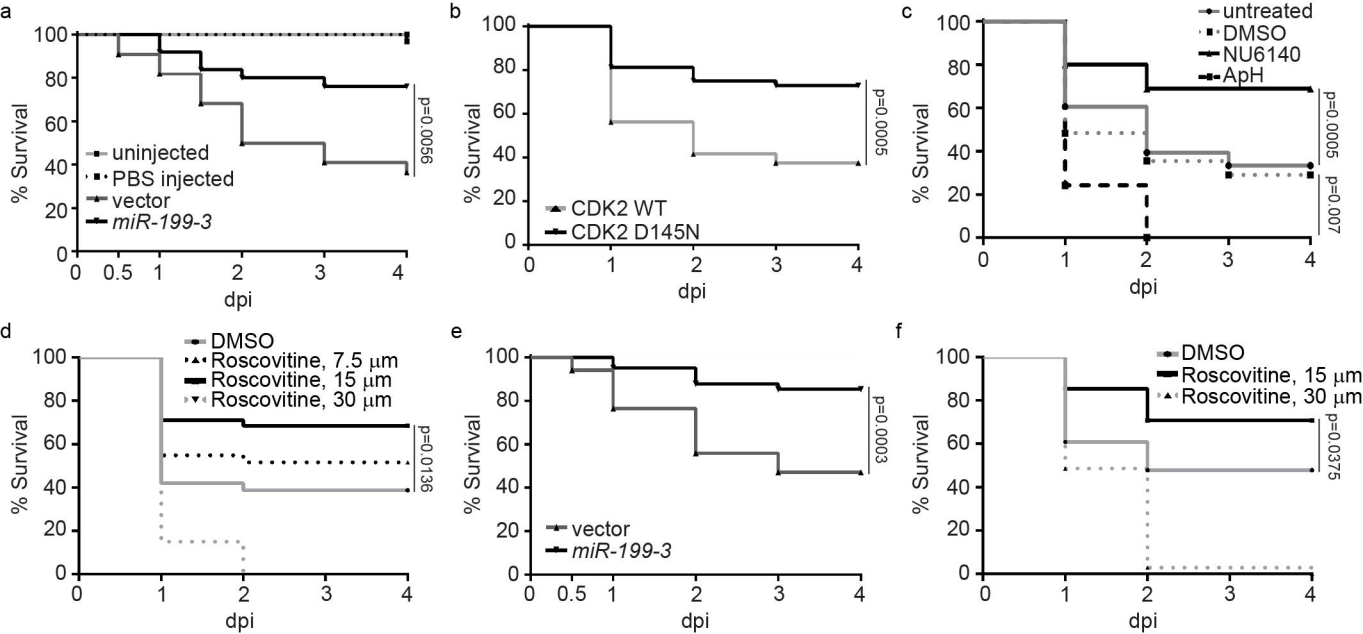
a
% Survival
dpi
uninjected
PBS injected
vector
miR-199-3
p=0.0056
b
CDK2 WT
CDK2 D145N
p=0.0005
c
untreated
DMSO
NU6140
ApH
p=0.0005
p=0.007
d
DMSO
Roscovitine, 7.5 μm
Roscovitine, 15 μm
Roscovitine, 30 μm
p=0.0136
e
vector
miR-199-3
p=0.0003
f
DMSO
Roscovitine, 15 μm
Roscovitine, 30 μm
p=0.0375